



Cite this: *J. Mater. Chem. B*, 2018, **6**, 1501

A photostable AIE luminogen with near infrared emission for monitoring morphological change of plasma membrane†

Weijie Zhang,[‡] Chris Y. Y. Yu,^{‡,ab} Ryan T. K. Kwok,^{ab} Jacky W. Y. Lam^{ab} and Ben Zhong Tang^{*abc}

The morphology of plasma membrane is dynamic and keeps changing in order to maintain its homeostasis. Abnormality in cell membrane shape could be viewed as a sign of unhealthy cells. A lipophilic cyanostilbene derivative (AS2CP-TPA) composed of a hydrophilic pyridinium salt and a hydrophobic triphenylamino group was designed for staining the cell membrane and monitoring membrane morphology under different conditions. Due to strong donor–acceptor interaction and aggregation-induced emission property, AS2CP-TPA emits weak emission in aqueous solution, but it lights up the plasma membrane of HeLa cells with near infrared fluorescence under an excitation wavelength of 460 nm. With merits of high photostability and high specificity to plasma membrane, AS2CP-TPA is capable of long-term monitoring of the morphological changes of cell membrane during Hg²⁺ and trypsin treatments.

Received 13th November 2017,
Accepted 9th February 2018

DOI: 10.1039/c7tb02947k

rsc.li/materials-b

Introduction

Plasma membrane is composed of a phospholipid bilayer with embedded proteins. Because of the selective permeability, it plays an important role in the regulation of substance exchange, and maintaining intracellular homeostasis. Cell membrane is involved in a variety of cellular processes, such as nutrient transport, signal transduction, endocytosis and exocytosis.^{1–3} Examination of the morphology of the plasma membrane can provide useful information to scientists to study the cell functions and metabolisms.^{4–6} For example, a pseudopodium forms on the plasma membrane to swallow pathogens during phagocytosis.⁷ Moreover, disruption of cell membrane can cause rapid depolarization, resulting in leakage of cell content and cell death. Thus, real-time monitoring of the dynamic morphological change of plasma membrane under

different circumstances is of critical importance in biomedical research and drug development.

Fluorescence spectroscopy is a powerful and reliable technique and has been extensively utilized to visualize intracellular structures with superior sensitivity and resolution. A fluorescent probe with high organelle-specificity and good image contrast is primarily required in order to acquire a good fluorescent image of the cellular structure. In recent decades, a variety of fluorescent materials with different properties and functionalities have been extensively developed. For example, inorganic quantum dots (QDs), because of their brightness and tunable color, have earned increasing research interests.^{8,9} However, the cytotoxicity of QDs is still unavoidable. Apart from inorganic fluorescent materials, several organic fluorescent dyes for biological imaging are also commercially available.⁹ In particular, CellMask is a series of fluorescent biomarkers for plasma membrane imaging. Although these dyes can selectively image the cell membrane with desirable brightness, their emission is easily bleached upon photo-excitation owing to their poor photostability and low working concentration. Unfortunately, this photostability problem cannot be solved using higher dose of dye as their emissions greatly weaken due to the aggregation-caused quenching (ACQ) effect.

When designing organelle-specific fluorescent probes for long-term monitoring of biological processes, photostability and brightness of the probes are the two important parameters that have to be taken into consideration. In past decades,

^a Hong Kong Branch of Chinese National Engineering Research Centre for Tissue Restoration and Reconstruction, Department of Chemistry, Institute for Advanced Study and Division of Life Science, The Hong Kong University of Science and Technology, Clear Water Bay, Kowloon, Hong Kong, China.
E-mail: tangbenz@ust.hk

^b HKUST Shenzhen Research Institute, No. 9 Yuexing First RD, South Area, Hi-tech Park, Nanshan, Shenzhen, 518057, China

^c NSFC Center for Luminescence from Molecular Aggregates, SCUT-HKUST Joint Research Laboratory, State Key Laboratory of Luminescent Materials and Devices, South China University of Technology, Guangzhou, 510640, China

† Electronic supplementary information (ESI) available: Characterization of AS2CP-TPA and intermediate. See DOI: 10.1039/c7tb02947k

‡ These authors contributed equally to this work.

luminogens with aggregation-induced emission (AIE) have attracted special research interests in the field of biological sensing, imaging and therapy because of their unique photo-physical properties.¹⁰ In general, they are practically non-emissive in molecular dissolved state, but emit intensively in aggregated and solid states.^{11,12} In contrast to emission quenching, the intensity of a fluorophore increases with an increase in the concentration. The higher the dose of AIE luminogen (AIEgen), the stronger will be the resultant emission. Owing to the nature of aggregates, AIE fluorescent probes always possess superior photostability, possibly due to the fact that only the surface of the aggregates is photo-bleached upon photo-excitation and molecules in the core of the aggregates can still emit. With rational design, researchers have developed various AIEgens for imaging and monitoring biological processes involving mitochondria, lysosome and lipid droplets.¹³ However, for plasma membrane staining, only few AIEgens have been reported. It is well known that cell membrane is formed by dense lipid bilayers with hydrophilic and hydrophobic parts.¹⁴ For designing a fluorescent bio-probe to specifically insert and long-term retain to the cell membrane, many characteristics of fluorescent molecules including molecular size, electrical charge and lipophilicity should be well devised to suit the unique special structure of cell membrane. Recently, Liang and Li *et al.* reported two AIE fluorescent probes to target plasma membrane, but they exhibit green emission at ~500 nm with UV excitation.^{15,16} For *in vitro* cell studies, luminogens with red emission are more favorable because it can minimize auto-fluorescence interference and optical self-absorption. Therefore, development of red/near infrared AIEgens with high photostability and good specificity to plasma membrane is of importance for real-time and long-term monitoring of the morphological change of plasma membrane.

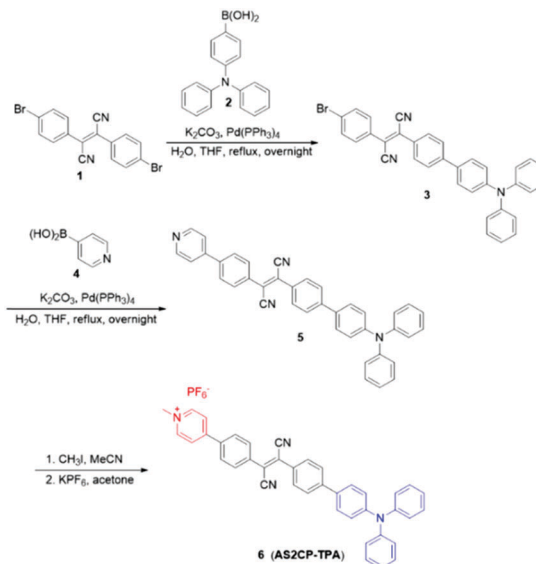
In this study, we designed and synthesized an AIE-active dicyanostilbene derivative with near infrared emission for cell membrane imaging and monitoring. In order to shift the absorption and emission wavelengths into the red region, the dicyanostilbene core was decorated with pyridinium and triphenylamine groups, which are electron donors and acceptors, respectively. The lipophilic structure aids the designed AIEgen to specifically image the plasma membrane. We also demonstrated that our AIEgen can monitor the morphological changes in the plasma membrane when HeLa cells were treated with Hg²⁺ and trypsin.

Results and discussion

Design and synthesis of AS2CP-TPA

Dicyanostilbene has been used commonly as a building block for developing orange/red AIEgens due to its intrinsic AIE characteristics and strong electron withdrawing property.

By decorating dicyanostilbene with different electron donating groups, AIEgens with long-wavelength emission can be readily synthesized.^{17,18} In consideration of the phospholipid bilayer structure of plasma membrane, a new dicyanostilbene-based



Scheme 1 The chemical structure of AS2CP-TPA and its synthetic route.

AIEgen (AS2CP-TPA) with balanced lipophilicity was designed and synthesized. The chemical structure of AS2CP-TPA is depicted in Scheme 1. It is composed of three components: (i) dicyanostilbene, which works as the AIE building block with strong electron-withdrawing ability (shown in black); (ii) hydrophobic triphenylamine group, which serves as a strong electron-donor group (shown in blue); (iii) positively-charged pyridinium (Py) salt, which acts as an electron-withdrawing group and endows water solubility to the designed AIEgen (shown in red). The synthetic procedure is denoted in Scheme 1. In brief, dibromo-substituted dicyanostilbene (1) was first coupled with 4-(diphenylamino)phenylboronic acid (2) in the presence of Pd(PPh₃)₄ and K₂CO₃ to afford compound 3 with reasonable yield. The intermediate 3 was further coupled with 4-pyridinylboronic acid (4) through Suzuki coupling to afford compound 5, which was then treated with iodomethane in acetonitrile and KPF₆ in acetone to afford the targeted compound 6 (AS2CP-TPA). AS2CP-TPA and all intermediates were characterized using NMR and high-resolution mass spectrometry (Fig. S1–S9, ESI[†]), from which satisfactory results corresponding to the structure of our compounds were obtained.

Optical properties

The photophysical properties of AS2CP-TPA were first investigated. AS2CP-TPA was soluble in polar solvents such as dimethyl sulfoxide (DMSO), while it had poor solubility in non-polar organic solvents such as toluene. It showed an absorption maximum at 460 nm in DMSO solution with molar absorptivity of 18 000 cm⁻¹ M⁻¹ (Fig. 1A). The absorption peak of AS2CP-TPA was bathochromically shifted by 100 nm as compared to that of dicyanostilbene, which could be reasonably explained by the fact that AS2CP-TPA has a stronger donor–acceptor interaction.¹⁶ To evaluate the AIE properties of AS2CP-TPA, photoluminescence (PL) of AS2CP-TPA in DMSO/toluene mixtures with different toluene fractions (*f*_t) was measured.

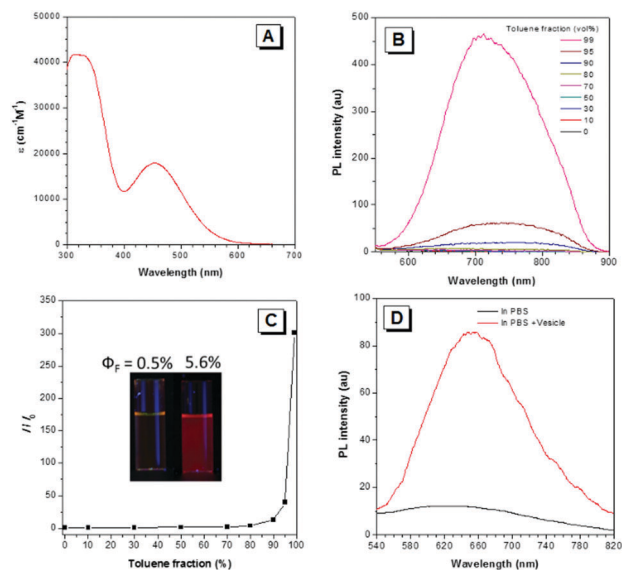


Fig. 1 (A) Absorption spectrum of AS2CP-TPA in DMSO solution. (B) PL spectra of AS2CP-TPA in DMSO/toluene mixtures with different toluene fraction (f_t). (C) Plot of I/I_0 versus f_t , where I and I_0 were the PL intensities of AS2CP-TPA recorded at 720 nm in DMSO/toluene mixtures with different f_t and in pure DMSO solution, respectively. Inset: Photographs of AS2CP-TPA in $f_t = 0\%$ (left) and 99% (right) taken under illumination of a hand-held UV lamp with 365 nm. (D) PL spectra of AS2CP-TPA in PBS solution with or without addition of lipid vesicle. Conditions: AS2CP-TPA concentration = 10 μM ; excitation wavelength = 460 nm.

In pure DMSO solution, AS2CP-TPA emitted very weak emission (Fig. 1B). No distinct change in emission intensity was observed when the f_t in the mixture was below 90%. Further addition of toluene into the mixture resulted in rapid growth in the PL intensity. At 99% f_t , the quantum efficiency of AS2CP-TPA was 5.6%, which was 11.2-fold higher compared to that in pure DMSO (Fig. 1C). The PL study suggested that AS2CP-TPA was molecularly dissolved when the f_t was below 90%, in which the intramolecular motion activated non-radiative decay and discouraged the relaxation in radiative channel. When excess toluene was added, the AS2CP-TPA molecules were forced to interact and form aggregates. In the aggregated state, the intramolecular motion of AS2CP-TPA was restricted, thus promoting the relaxation of excitation energy in radiative channels.¹⁰

Can AS2CP-TPA also generate favourable red emission in plasma membrane? Before the cell staining experiments, we tried to mimic the conditions in plasma membrane by fabricating lipid vesicles with different compositions of phospholipid.^{19,20} As shown in Fig. 1D, AS2CP-TPA gave only weak emission in phosphate-buffered saline (PBS), possibly as the Py group endowed good water solubility to AS2CP-TPA. In the presence of lipid vesicles, distinct emission of AS2CP-TPA in PBS was observed. This experimental result encouraged us to explore the possibility of AS2CP-TPA as a fluorescent visualizer for plasma membrane imaging. Notably, the emission of AS2CP-TPA in lipid vesicles was relatively blue-shifted (about 70 nm) as compared to the aggregates formed in the mixture of DMSO/toluene with high f_t , which could be explained by the fact that the vesicles provide

less polar environment for AS2CP-TPA molecules and thus, the emission was blue shifted as a result of TICT effect.²¹

Plasma membrane imaging and photostability

Biocompatibility is an important parameter to determine whether a fluorophore is suitable for use in bioimaging. Thus, we evaluated the cytotoxicity of AS2CP-TPA by MTT assay before employing it in cell imaging. The cell viabilities of HeLa cells were all above 80% after incubating AS2CP-TPA in the concentration ranging from 0–10 μM (Fig. 2A), suggesting that AS2CP-TPA possesses low cytotoxicity and hence, it is suitable for imaging applications.

Furthermore, to evaluate the selectivity of AS2CP-TPA to plasma membrane, a commercial biomarker, namely, CellMask Green Plasma Membrane was used to co-stain the HeLa cells with AS2CP-TPA. As shown in confocal images in Fig. 2B–D, the red fluorescence of AS2CP-TPA was primarily located on the plasma membrane of HeLa cells and it effectively overlapped with the green fluorescent signal from CellMask Green Plasma Membrane, indicating that AS2CP-TPA was plasma membrane-specific. To further verify whether the AS2CP-TPA only stained the plasma membrane, we gained the 3D structure of the dye-stained HeLa cells by scanning different layers using a confocal microscope. By carefully examining the scanned images (Fig. 2E and Video S1 in ESI[†]), the fine structure of the membrane was effectively visualized and no fluorescence was detected in the cytoplasmic components of HeLa cells. All of these results illustrated that AS2CP-TPA can stain the plasma membrane as specifically as the commercial CellMask Green Plasma Membrane biomarker.

In order to monitor biological processes occurring in the plasma membrane, fluorescent probes with high photostability are required as the dye-stained cells are scanned many times. We quantitatively investigated the photostability of AS2CP-TPA in the dye-stained HeLa cells by continuous scanning under a confocal microscope and compared the data with that obtained for CellMask Deep Red Plasma Membrane. Under the same

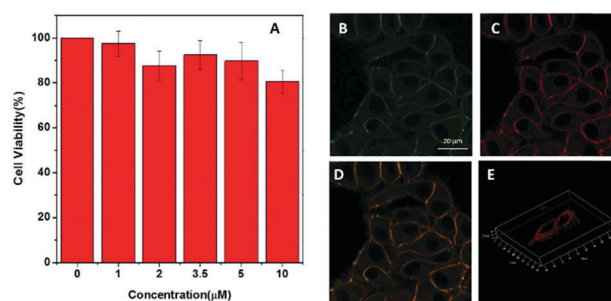


Fig. 2 (A) Cell viability of HeLa cells incubated with AS2CP-TPA at different concentrations for 12 h. Data was expressed as mean value for five separate trials. (B–D) Confocal images of HeLa cells co-stained with AS2CP-TPA (3.5 μM) and CellMask Green Plasma Membrane (5 ng mL^{-1}) for 5 min. Conditions: (B) λ_{ex} : 526 nm and λ_{em} : 600–700 nm for AS2CP-TPA; (C) λ_{ex} : 488 nm and λ_{em} : 500–540 nm for CellMask Green Plasma Membrane. (D) The merge images of (B) and (C). (E) 3D confocal images of AS2CP-TPA stained HeLa cells gained by scanning different layers. Condition: λ_{ex} : 488 nm and λ_{em} : 600–750 nm.

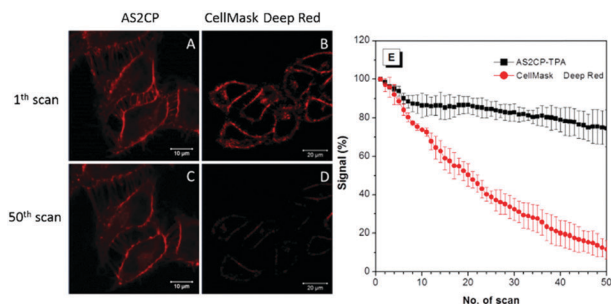


Fig. 3 Confocal images of HeLa cells stained with (A and C) AS2CP-TPA ($3.5 \mu\text{M}$) or (B and D) CellMask Deep Red Plasma Membrane (5 ng mL^{-1}) taken under continuous light excitation. (E) Plot of fluorescent signal (%) from HeLa cells stained with AS2CP-TPA (black) or CellMask Deep Red Plasma Membrane (red) with increasing number of scans. Conditions: $\lambda_{\text{ex}} = 488 \text{ nm}$ and $\lambda_{\text{em}} = 600\text{--}750 \text{ nm}$ for AS2CP-TPA; $\lambda_{\text{ex}} = 560 \text{ nm}$, $\lambda_{\text{em}} = 600\text{--}700 \text{ nm}$ for CellMask Deep Red Plasma Membrane.

excitation power, about 20% of AS2CP-TPA fluorescent signal was lost after 50 scans. In sharp contrast, the fluorescence of the CellMask Deep Red Plasma Membrane was almost quenched and the plasma membrane was very difficult to observe (Fig. 3D and E). This is a formidable problem for commercial dyes, due to which they are not capable of monitoring the biological process occurring in the cells.²² In contrast, AS2CP-TPA benefited in high resistance to photo-oxidation; thus, it is favourable to be used in monitoring of plasma membrane morphology.

Morphology changes in plasma membrane

Abnormal morphology change of plasma membrane is closely related to the health of the cells,^{23,24} however, its dynamic changes under different conditions are rarely recorded. As AS2CP-TPA can selectively stain plasma membrane in live cells with superior photostability, we attempted to apply it for monitoring the changes in plasma membrane morphology under different circumstances. Hg^{2+} is one of the most toxic chemicals for health of human beings. It can cause cell dysfunction and induce cell death.²⁵ Hua *et al.* has reported that Hg^{2+} can induce bleb formation on plasma membrane.²⁶ Thus, we incubated AS2CP-TPA stained HeLa cells in the presence of Hg^{2+} and continuously monitored the plasma membrane morphology under a confocal microscope. The confocal images (Fig. 4A and B) show that the HeLa cells were stained with AS2CP-TPA and treated with Hg^{2+} for 0 min (pseudo red) and 40 min (pseudo green), respectively. A bleb was observed, implicating that the Hg^{2+} interacted with cytoskeleton as a result of actin filament disruption. When the actin filament was damaged, the hydrostatic pressures in the disrupted sites increased and forced the bilayer membrane out. To confirm that the bleb formation was not due to the actions of AS2CP-TPA, a control experiment was conducted by treating the dye-stained cells without Hg^{2+} . In the absence of Hg^{2+} , the morphology of plasma membrane did not show distinct change after long incubation time (Fig. 4C and D). This experiment showed that AS2CP-TPA can possibly monitor the morphological changes of plasma membrane under toxic conditions.

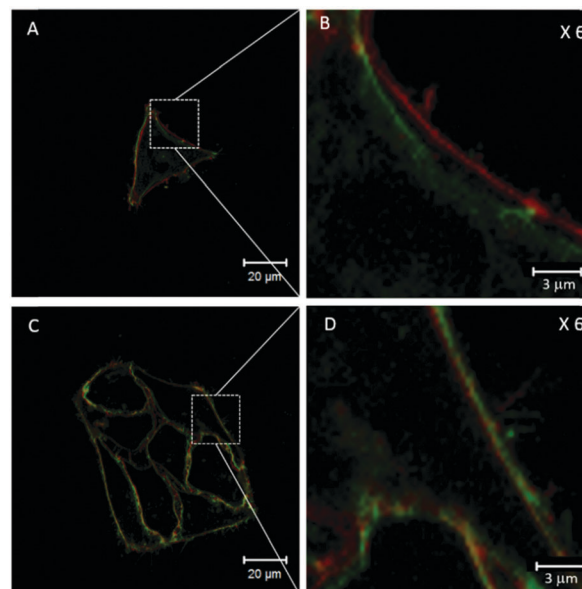


Fig. 4 Overlaid confocal images of AS2CP-TPA-stained HeLa cells before (pseudo red) and after (pseudo green) incubation in PBS containing $100 \mu\text{M}$ Hg^{2+} for 40 min (A and B) or incubation in PBS only for 40 min (C and D). Conditions: $\lambda_{\text{ex}} = 488 \text{ nm}$ and $\lambda_{\text{em}} = 600\text{--}750 \text{ nm}$.

Cell adhesion, a process of interaction and attachment of a cell into a substrate surface, has been widely used in biological experiments.²⁷ The interaction is driven by the action of cell adhesion molecules (CAMs), which are glycoproteins, on the cell surface and bind to the extracellular matrix.^{27,28} In the process of adhesion on coverslips, the shape of cells changes from sphere to flat. Moreover, the adherent cells can be detached by treating with trypsin, which is a protease used to cleave the peptide bonds of CAMs. If CAMs are digested by trypsin, the adherent cells will leave the substrate surface and the detached cells will recover their spherical shape (Scheme S1, ESI†).

Through this speculation, we explored the possibility to use AS2CP-TPA to monitor the process of the detachment of the adherent cells. We first imaged the adherent cells stained with AS2CP-TPA using confocal microscope (Fig. 5A). After addition of trypsin, the fluorescent images were recorded at different time interval (Fig. 5B–H). At 0 min, the cell appeared to be flat. As the time passed on, the cells appeared spherical, suggesting

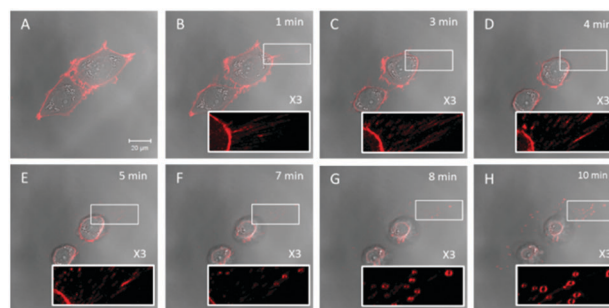


Fig. 5 Confocal images of AS2CP-TPA-stained HeLa cells incubated with trypsin for 0–10 min. Conditions: $\lambda_{\text{ex}}: 488 \text{ nm}$ and $\lambda_{\text{em}}: 600\text{--}750 \text{ nm}$.

that the cells detached from the coverslip. More interestingly, some spherical vesicles surrounded the cells were observed after 7 min. We propose that these vesicles were caused by disassociation of the bilayer membrane during cell detachment. Since the membrane is composed of bilayer phospholipid, the destroyed membranes tend to form micelles in the aqueous environment. Nevertheless, this result suggests that AS2CP-TPA is a potential candidate for long-term monitoring of morphological changes of the plasma membrane and probing micro-events such as micelle formation.

Conclusions

In summary, a lipophilic AIEgen with near-infrared emission, namely, AS2CP-TPA was designed and synthesized. Apart from possessing long-wavelength absorption and emission, AS2CP-TPA also showed high biocompatibility, high photostability and high specificity to the plasma membrane. These advantages are beneficial for long-term monitoring of the morphological changes of plasma membrane under different circumstances, such as treatment of live cells with Hg^{2+} or detachment of adherent cells by trypsin. AS2CP-TPA is a promising candidate to be used in the plasma membrane-related studies.

Experimental

Materials and instruments

THF (Labscan) was purified by simple distillation from sodium benzophenone ketyl under nitrogen immediately before use. Synthetic lipids, DOPC (1,2-dioleoyl-*sn*-glycero-4-phosphocholine), TOCL (1,1',2,2'-tetraoleoyl cardiolipin), DOPS (1,2-dioleoyl-*sn*-glycero-3-phospho-L-serine (sodium salt)), DPPE (1,2-dipalmitoleoyl-*sn*-glycero-3-phosphoethanolamine) and soy PI (*L*- α -phosphatidylinositol (Soy) (sodium salt)) were purchased from Avanti Polar Lipids, Inc. (Alabaster, AL). SM (*N*-hexanoyl-D-sphingomyelin), 4-(diphenylamino)phenylboronic acid, 4-bromophenylacetonitrile and 4-pyridinylboronic acid were purchased from Sigma. Water was purified by a Millipore filtration system. All the experiments were performed at room temperature unless otherwise specified.

^1H and ^{13}C NMR spectra were recorded on a Bruker AV 400 spectrometer in CDCl_3 and $\text{DMSO}-d_6$ using tetramethylsilane (TMS; $\delta = 0$) as internal reference. Absorption spectra were recorded on a Varian Cary 50 UV-Vis spectrophotometer. Steady-state fluorescence spectra were recorded on a Perkin-Elmer LS 55 spectrofluorometer with a Xenon discharge lamp excitation. Mass spectra were recorded on a GCT Premier CAB 048 mass spectrometer operated in MALDI-TOF mode. Fluorescent images were collected on an Olympus BX 41 fluorescence microscope. Laser confocal scanning microscope images were collected on Zeiss laser scanning confocal microscope (LSM7 DUO) and analysed using ZEN 2009 software (Carl Zeiss).

Synthesis

Bis(4-bromophenyl)fumaritrile (1) was synthesized according to the method described in a previous report.¹⁸ AS2CP-TPA was prepared according to the synthetic route shown in Scheme 1.

Synthesis of compound 3. Into a 100 mL two-necked round bottom flask equipped a condenser, bis(4-bromophenyl)fumaritrile (1; 300 mg, 0.77 mmol), 4-(diphenylamino)phenylboronic acid (2; 200 mg, 0.70 mmol), potassium carbonate (1.07 g, 7.73 mmol) and $\text{Pd}(\text{PPh}_3)_4$ (27 mg, 0.023 mmol), dissolved in 35 mL distilled THF and 8 mL degassed water, were added under nitrogen. The mixture was heated to reflux overnight. After being cooled to room temperature, the mixture was extracted with dichloromethane (DCM) three times. The organic phase was combined and washed with water and then dried over anhydrous sodium sulphate. After filtration and evaporation of organic solvents, the crude product was purified by silica gel column chromatography using *n*-hexane/DCM (*v/v* = 7:3) as eluent. Orange solid was obtained. Yield: 56%. ^1H NMR (400 MHz, CDCl_3), δ (ppm): 7.94 (d, 2H, *J* = 8.4 Hz), 7.74 (d, 2H, *J* = 8.4 Hz), 7.70–7.69 (m, 3H), 7.54 (d, 2H, *J* = 8.8 Hz), 7.32–7.28 (m, 5H), 7.17 (d, 6H, *J* = 8.4 Hz), 7.08 (t, 2H, *J* = 7.2 Hz). ^{13}C NMR (100 MHz, CDCl_3), δ (ppm): 146.7, 131.9, 123.0, 128.8, 128.6, 127.2, 126.4, 124.3, 122.9, 122.5. HRMS (MALDI-TOF): *m/z*: 553.1021 (M^+ , calcd 553.0977).

Synthesis of compound 5. Into a 100 mL two-necked round bottom flask equipped with a condenser, compound 3 (170 mg, 0.31 mmol), 4-pyridinylboronic acid (4; 45 mg, 0.37 mmol), potassium carbonate (430 mg, 3.08 mmol) and $\text{Pd}(\text{PPh}_3)_4$ (11 mg, 0.0092 mmol), dissolved in 25 mL THF and 3 mL degassed water, were added under nitrogen. The mixture was stirred and heated to reflux overnight. After cooling to room temperature, the mixture was extracted with DCM three times. The organic phase was collected, washed with water and dried over anhydrous sodium sulphate. After filtration and solvent evaporation, the crude product was purified by silica-gel column chromatography using DCM/ethyl acetate (*v/v* = 99:1) as eluent to furnish an orange solid as the product. Yield: 74%. ^1H NMR (400 MHz, CDCl_3), δ (ppm): 8.75 (d, 2H, *J* = 4.0 Hz), 7.99–7.95 (m, 4H), 7.83 (d, 2H, *J* = 8.4 Hz), 7.76 (d, 2H, *J* = 8.4 Hz), 7.58 (d, 2H, *J* = 5.6 Hz), 7.54 (d, 2H, *J* = 8.4 Hz), 7.30 (t, 4H, *J* = 8.0 Hz), 7.17 (d, 6H, *J* = 8.4 Hz), 7.08 (t, 2H, *J* = 7.2 Hz). ^{13}C NMR (100 MHz, CDCl_3), δ (ppm): 149.7, 146.7, 146.6, 131.7, 129.6, 129.4, 129.0, 128.8, 128.7, 127.2, 127.0, 126.4, 124.3, 122.9, 122.5. HRMS (MALDI-TOF): *m/z*: 550.2115 (M^+ , calcd 550.2157).

Synthesis of compound 6 (AS2CP-TPA). Into a 100 mL two-necked round bottom flask equipped with a condenser, compound 5 (50 mg, 0.154 mmol), dissolved in 5 mL acetonitrile, was added. Iodomethane (0.1 mL) was then added and the mixture was heated to reflux for 8 h. After cooling to room temperature, the mixture was poured into diethyl ether. Dark red precipitates were formed and filtered by suction filtration. The precipitates were re-dissolved in acetone and mixed with saturated KPF6 solution (5 mL). After stirring for 1 h, acetone was evaporated by compressed air. The dark red precipitates were filtered, washed with water and dried under reduced

pressure. Yield: 95%. ^1H NMR (400 MHz, $\text{DMSO-}d_6$), δ (ppm): 9.01 (d, 2H, $J = 6.8$ Hz), 8.54 (d, 2H, $J = 6.8$ Hz), 8.28 (d, 2H, $J = 8.4$ Hz), 8.10 (d, 2H, $J = 8.4$ Hz), 7.96–7.89 (m, 4H), 7.73 (d, 2H, $J = 8.8$ Hz), 8.34 (d, 4H, $J = 7.6$ Hz), 7.11–7.01 (m, 8H), 4.33 (s, 3H). ^{13}C NMR (100 MHz, $\text{DMSO-}d_6$), δ (ppm): 146.5, 146.4, 145.4, 130.0, 129.8, 129.6, 129.3, 127.7, 127.5, 126.4, 124.4, 124.3, 123.7, 122.2. HRMS (MALDI-TOF): m/z : 565.2332 (M^+ , calcd 565.2392).

Cell culture

HeLa cells were cultured in MEM supplemented with 10% heat-inactivated FBS, 100 unit per mL penicillin and $100 \mu\text{g mL}^{-1}$ streptomycin in a humidity incubator with 5% CO_2 at 37 °C. Before the experiment, the HeLa cells were pre-cultured until confluence was attained.

Cytotoxicity study

To evaluate the cytotoxicity of AS2CP-TPA, 2-(4,5-dimethyl-2-thiazolyl)-2,5-diphenyltetrazolium bromide (MTT) assay was employed. HeLa cells (provided by American Type Culture Collection) were seeded in a 96-well plate at a density of 5000 cells per well. After 24 h of incubation, the cells were exposed to a series of doses of AS2CP-TPA (0–5 μM) in culture medium at 37 °C. One day later, 10 μL of freshly prepared MTT solution was added into each well. After further incubation for 8 h, 100 μL of solubilization solution containing 10% SDS and 0.01 M HCl was added to dissolve the purple crystals. Two hours later, the absorbance at 595 nm was recorded using a Perkin-Elmer Victor plate reader. The experiment was performed at least five times.

Cell imaging

HeLa cells were seeded on a 35 mm Petri dish with a glass cover slide. After overnight cell culture, the HeLa cells were incubated in an aqueous solution of AS2CP-TPA (3.5 μM) or CellMask Deep Red Plasma Membrane (5 ng mL^{-1}) for 5 min. The dye labelled-cells were washed with fresh phosphate buffered saline (PBS; pH 7.4) three times before fluorescent imaging. For co-staining experiments, a solution of CellMask Green Plasma Membrane (5 ng mL^{-1}) was added to the HeLa cells incubated with an aqueous solution of AS2CP-TPA (3.5 μM). After further incubation for 5 min, the dye-labelled cells were washed with fresh PBS solution three times and then imaged by wide-field fluorescence and confocal microscopies.

Preparation of lipid vesicles

Chloroform stocks of different lipids (10 mg mL^{-1}) were mixed in a desired molar ratio and dried under a stream of nitrogen. The lipid films were hydrated in 25 mM HEPES buffer (pH 7.4) to a final lipid concentration of 2.2 mM. The lipid mixtures were incubated for 30 min at 37 °C and then sonicated for 1 h. The lipid vesicles were obtained by extruding the lipid mixtures 11 times through 100 nm pore size polycarbonate filter at 50 °C on a pre-warmed lipid extruder.^{29,30}

Photostability test

Live dye-labelled HeLa cells were imaged on a confocal microscope. Conditions: excitation wavelength: 526 nm and emission filter: 600–750 nm (AS2CP-TPA); excitation wavelength: 560 nm and emission filter: 600–700 nm (CellMask Deep Red Plasma Membrane).

Conflicts of interest

There are no conflicts to declare.

Acknowledgements

This study was partially supported by the Innovation and Technology Commission (ITC-CNERC14SC01), the National Science Foundation of China (21788102) the National Basic Research Program of China (2013CB834701 and 2013CB834702), and the Research Grants Council of Hong Kong (16301614, 16305015, 16308016, N_HKUST604/14 and A-HKUST605/16). B. Z. T. is also grateful for the support from the Science and Technology Plan of Shenzhen (JCYJ201602229205601482) and AIEgen Biotech Co., Ltd for their supports in materials.

Notes and references

- J. Schlessinger, D. Axelrod, D. Koppel, W. Webb and E. Elson, *Science*, 1977, **195**, 307.
- S. Grimmer, B. van Deurs and K. Sandvig, *J. Cell Sci.*, 2002, **115**, 2953.
- J. Rejman, V. Oberle, I. S. Zuhorn and D. Hoekstra, *Biochem. J.*, 2004, **377**, 159.
- R. F. Zwaal and A. J. Schroit, *Blood*, 1997, **89**, 1121.
- B. Fadeel and D. Xue, *Crit. Rev. Biochem. Mol. Biol.*, 2009, **44**, 264.
- J. Gutknecht, *J. Membr. Biol.*, 1981, **61**, 61.
- D. M. Underhill and H. S. Goodridge, *Nat. Rev. Immunol.*, 2012, **12**, 492.
- X. Michalet, F. F. Pinaud, L. A. Bentolila, J. M. Tsay, S. Doose, J. J. Li, G. Sundaresan, A. M. Wu, S. S. Gambhir and S. Weiss, *Science*, 2005, **307**, 538.
- U. Resch-Genger, M. Grabolle, S. Cavaliere-Jaricot, R. Nitschke and T. Nann, *Nat. Methods*, 2008, **5**, 763.
- J. Mei, N. L. C. Leung, R. T. K. Kwok, J. W. Y. Lam and B. Z. Tang, *Chem. Rev.*, 2015, **115**, 11718.
- J. Yang, L. Li, Y. Yu, Z. Ren, Q. Peng, S. Ye, Q. Lia and Z. Li, *Mater. Chem. Front.*, 2017, **1**, 91.
- C. Wang and Z. Li, *Mater. Chem. Front.*, 2017, **1**, 2174.
- H. Fang and B. Liu, *Org. Biomol. Chem.*, 2016, **14**, 9931.
- D. Lingwood and K. Simons, *Science*, 2010, **327**, 46.
- C. Zhang, S. Jin, K. Yang, X. Xue, Z. Li, Y. Jiang, W.-Q. Chen, L. Dai, G. Zou and X.-J. Liang, *ACS Appl. Mater. Interfaces*, 2014, **6**, 8971.
- Y. Li, Y. Wu, J. Chang, M. Chen, R. Liu and F. Li, *Chem. Commun.*, 2013, **49**, 11335.

- 17 C. Y. Y. Yu, H. Xu, S. Ji, R. T. K. Kwok, J. W. Y. Lam, X. Li, S. Krishnan, D. Ding and B. Z. Tang, *Adv. Mater.*, 2017, **29**, 201606167.
- 18 X. Y. Shen, Y. J. Wang, E. Zhao, W. Z. Yuan, Y. Liu, P. Lu, A. Qin, Y. Ma, J. Z. Sun and B. Z. Tang, *J. Phys. Chem. C*, 2013, **117**, 7334.
- 19 G. van Meer, D. R. Voelker and G. W. Feigenson, *Nat. Rev. Mol. Cell Biol.*, 2008, **9**, 112.
- 20 D. A. Brown and E. London, *J. Biol. Chem.*, 2000, **275**, 17221.
- 21 R. Hu, E. Lager, A. Aguilar-Aguilar, J. Liu, J. W. Y. Lam, H. H. Y. Sung, I. D. Williams, Y. Zhong, K. S. Wong, E. Pena-Cabrera and B. Z. Tang, *J. Phys. Chem. C*, 2009, **113**, 15845.
- 22 L. Li, X. Shen, Q. H. Xu and S. Q. Yao, *Angew. Chem., Int. Ed.*, 2013, **52**, 424.
- 23 M. van Engeland, F. C. Ramaekers, B. Schutte and C. P. Reutelingsperger, *Cytometry*, 1996, **24**, 131.
- 24 K. Simons and E. Ikonen, *Nature*, 1997, **387**, 569.
- 25 F. Zahir, S. J. Rizwi, S. K. Haq and R. H. Khan, *Environ. Toxicol. Pharmacol.*, 2005, **20**, 351.
- 26 J. Heo, F. Meng, F. Sachs and S. Z. Hua, *Cell Biochem. Biophys.*, 2008, **51**, 21.
- 27 R. O. Hynes, *Cell*, 1992, **69**, 11.
- 28 G. M. Edelman, *Science*, 1983, **219**, 450.
- 29 C. W. T. Leung, Y. Hong, J. Hanske, E. Zhao, S. Chen, E. V. Pletneva and B. Z. Tang, *Anal. Chem.*, 2013, **86**, 1263.
- 30 J. E. Vance and D. Vance, *Biochemistry of Lipids and Membranes*, Elsevier Science, 2008.